

Holocene thinning of the Greenland ice sheet

B. M. Vinther¹, S. L. Buchardt¹, H. B. Clausen¹, D. Dahl-Jensen¹, S. J. Johnsen¹, D. A. Fisher², R. M. Koerner^{2,†}, D. Raynaud³, V. Lipenkov⁴, K. K. Andersen¹, T. Blunier¹, S. O. Rasmussen¹, J. P. Steffensen¹ & A. M. Svensson¹

On entering an era of global warming, the stability of the Greenland ice sheet (GIS) is an important concern¹, especially in the light of new evidence of rapidly changing flow and melt conditions at the GIS margins². Studying the response of the GIS to past climatic change may help to advance our understanding of GIS dynamics. The previous interpretation of evidence from stable isotopes ($\delta^{18}\text{O}$) in water from GIS ice cores was that Holocene climate variability on the GIS differed spatially³ and that a consistent Holocene climate optimum—the unusually warm period from about 9,000 to 6,000 years ago found in many northern-latitude palaeoclimate records⁴—did not exist. Here we extract both the Greenland Holocene temperature history and the evolution of GIS surface elevation at four GIS locations. We achieve this by comparing $\delta^{18}\text{O}$ from GIS ice cores^{3,5} with $\delta^{18}\text{O}$ from ice cores from small marginal icecaps. Contrary to the earlier interpretation of $\delta^{18}\text{O}$ evidence from ice cores^{3,6}, our new temperature history reveals a pronounced Holocene climatic optimum in Greenland coinciding with maximum thinning near the GIS margins. Our $\delta^{18}\text{O}$ -based results are corroborated by the air content of ice cores, a proxy for surface elevation⁷. State-of-the-art ice sheet models are generally found to be underestimating the extent and changes in GIS elevation and area; our findings may help to improve the ability of models to reproduce the GIS response to Holocene climate.

Ice cores from six locations^{3,8} have now been synchronized to the Greenland Ice Core Chronology 2005 (GICC05) throughout the

Holocene epoch (Fig. 1a). The GICC05 annual layer counting was performed simultaneously on the DYE-3, GRIP and NGRIP ice cores for the entire Holocene^{9,10}. For the Agassiz¹¹, Renland¹¹ and Camp Century ice cores the timescale was transferred by using volcanic markers identifiable in electrical conductivity measurements¹² (Supplementary Information). The six synchronized Holocene $\delta^{18}\text{O}$ records show large differences in millennial scale trends (Fig. 1b). All $\delta^{18}\text{O}$ records were obtained in the same laboratory (the Copenhagen Isotope Laboratory), ensuring maximum confidence in the homogeneity of the data sets. The differences are therefore real features that need to be understood and explained before firm conclusions about the evolution of Greenland climate during the Holocene can be supported by the data.

Changes in regional temperatures, moisture source regions, moisture transport and precipitation seasonality affect the $\delta^{18}\text{O}$ of precipitation⁶. However, all these parameters are expected to produce regional patterns of change, implying that trends in nearby $\delta^{18}\text{O}$ records should always be similar, except where the records are heavily influenced by a combination of ice flow and post-deposition phenomena, such as wind-scouring. Ice cores from Agassiz and Renland are retrieved from icecap domes and are therefore not influenced by ice flow. The Camp Century site is only slightly affected by a steady ice flow, yet the trends in the neighbouring Agassiz and Camp Century cores are dissimilar; in fact, the $\delta^{18}\text{O}$ signal at Agassiz is much more similar to the signal recorded at Renland on the other side of the GIS.

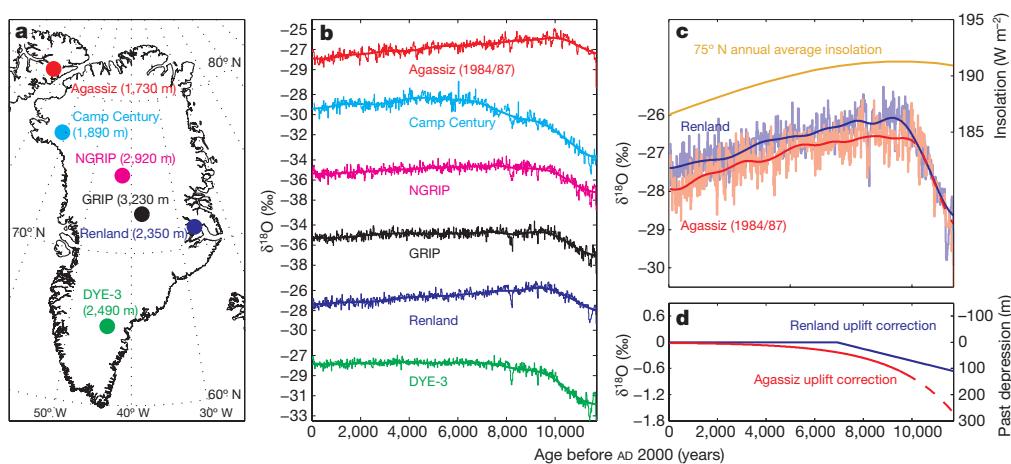


Figure 1 | Holocene $\delta^{18}\text{O}$ records. **a**, Drill site locations for the ice cores that have been cross-dated to the GICC05 timescale. Site elevations are given in parenthesis. **b**, 20-year averages and millennial scale trends of $\delta^{18}\text{O}$ during the Holocene as observed in ice core records from six locations in Greenland and Canada. All $\delta^{18}\text{O}$ values are expressed with respect to Vienna standard

mean ocean water (V-SMOW). **c**, Uplift-corrected Renland and Agassiz Holocene $\delta^{18}\text{O}$ values: 20-year averages and millennial scale trends in the Agassiz and Renland Holocene $\delta^{18}\text{O}$ records. Annual average insolation at 75°N is shown in orange. **d**, Agassiz and Renland post-glacial bedrock uplift histories and corresponding $\delta^{18}\text{O}$ correction values.

¹Centre for Ice and Climate, Niels Bohr Institute, University of Copenhagen, Juliane Maries Vej 30, DK-2100 Copenhagen Oe, Denmark. ²Glaciology Section, Terrain Sciences Division, Geological Survey of Canada, 601 Booth Street, Ottawa, Ontario, Canada K1A 0E8. ³Laboratoire de Glaciologie et Géophysique de l'Environnement, CNRS/UJF, BP 96, 38402 Saint-Martin-d'Hères, France. ⁴Arctic and Antarctic Research Institute, 38 Bering Street, St Petersburg 199397, Russia.

†Deceased.

Given the dissimilarity of some neighbouring $\delta^{18}\text{O}$ records, a more likely cause of the differences in $\delta^{18}\text{O}$ trends is past changes in the elevation of the GIS. Elevation change influences trends in the $\delta^{18}\text{O}$ records (Supplementary Information), and the differences in the long-term $\delta^{18}\text{O}$ trends seem to be related to changing GIS elevation: the pairs of records from the centre of the ice sheet (GRIP and NGRIP), those closer to the margin of the ice sheet (DYE-3 and Camp Century) and those from the small icecaps close to the GIS (Agassiz and Renland) are all similar.

For the GIS ice core records, the hypothesis that elevation change affected $\delta^{18}\text{O}$ in the past is difficult to evaluate, because little is known of the elevation history of the GIS. Ice sheet modelling is of little help because modelled elevation histories for GIS are highly dependent on poorly known boundary conditions, such as the past positions of the GIS margin¹³. However, for the small Agassiz and Renland icecaps it is possible to reconstruct past elevation histories with some confidence. Neither of these icecaps is believed to have experienced significant change in ice sheet thickness during most of the Holocene as a result of topographical constraints and the limited thickness of the icecaps^{8,14} (Supplementary Information). Both the Renland and the Agassiz bedrocks have experienced a significant post-glacial uplift. For Renland the uplift resulted from the retreat of the GIS, whereas the Agassiz uplift was caused by the disintegration of the Innuitian ice sheet that covered most of the Queen Elizabeth Islands during the last glaciation¹⁵. For both locations robust estimates of bedrock elevation have been obtained through studies of past changes in sea level in nearby fjords^{15,16}. The elevation history of the Renland bedrock is based on such studies throughout the Holocene, whereas that of the Agassiz bedrock is based on data sets back to 9.5 kyr before AD 2000. For the period from 9.5 kyr ago back to 11.7 kyr ago Agassiz bedrock elevation can be estimated by extrapolation, using the observed exponential half-life for the bedrock elevation change in the period 0–9.5 kyr before AD 2000 (ref. 17). If we assume that Agassiz and Renland $\delta^{18}\text{O}$ records have not been significantly influenced by changes in ice thickness during the Holocene, it is possible to correct the $\delta^{18}\text{O}$ records for past elevation changes, simply by using their respective bedrock elevation histories and the observed Greenland $\delta^{18}\text{O}$ –height relationship (Fig. 1c, d, and Supplementary Information).

The similarity between the uplift-corrected Agassiz and Renland $\delta^{18}\text{O}$ records is astounding given that the two icecaps are separated by about 1,500 km and by the entire GIS. The similarity suggests that

Greenland climate during the Holocene was homogeneous, with the same millennial-scale $\delta^{18}\text{O}$ evolution both east and northwest of the ice sheet. The homogeneous climatic history for the Greenlandic region is probably related to the regional change in solar insolation¹⁸, at least for the past 10 kyr.

Given the similarity of the Agassiz and Renland elevation-corrected $\delta^{18}\text{O}$ records, we assume that their common millennial-scale $\delta^{18}\text{O}$ trends would have been present in the ice cores from the GIS if the GIS had not changed surface elevation. The elevation histories for the four drill sites on the GIS (Fig. 2a) can then be estimated from the changes in difference between $\delta^{18}\text{O}$ records from the GIS sites and uplift-corrected $\delta^{18}\text{O}$ records from the two adjacent icecaps. The changes in elevation seen in Fig. 2a are corrected for upstream effects due to ice flow at the drill sites^{19,20} (Supplementary Information), thus showing changes in GIS elevation at the locations of the four drill sites. The derivation of the uncertainty bands for the changes in GIS elevation shown in Fig. 2a is discussed in the Supplementary Information.

From Fig. 2a it is seen that the initial response of the GIS to Holocene climatic conditions was a slight increase in elevation at all locations right after the onset of the Holocene (most probably in response to increased precipitation and bedrock uplift). Next the GIS responded to the effects of increased melt at the margins and ice break-off because of rising sea level. The melt and ice break-off induced rapid thinning at the Camp Century and DYE-3 sites, which are located relatively close to the margin. Then the thinning process propagated slowly towards the centre of the GIS, reaching GRIP at the present summit about 4,000 years after the onset of the Holocene.

The total gas content of air bubbles trapped in the ice is the only other known parameter in ice cores that is significantly and directly influenced by elevation change. A comparison between the elevation histories for GRIP and Camp Century and their total gas content records^{7,21} (Fig. 2b) shows an excellent qualitative agreement between past elevation change and change in total gas content. A detailed quantitative study of the differences between Camp Century and GRIP elevation and total gas content histories also yields strong support for the isotope-based elevation histories (Supplementary Information).

Figure 2c shows a reconstruction of the evolution of Greenland temperatures during the Holocene. This temperature reconstruction is based on Agassiz and Renland average $\delta^{18}\text{O}$ values, corrected for uplift and changes in $\delta^{18}\text{O}$ content of the ocean²². The conversion

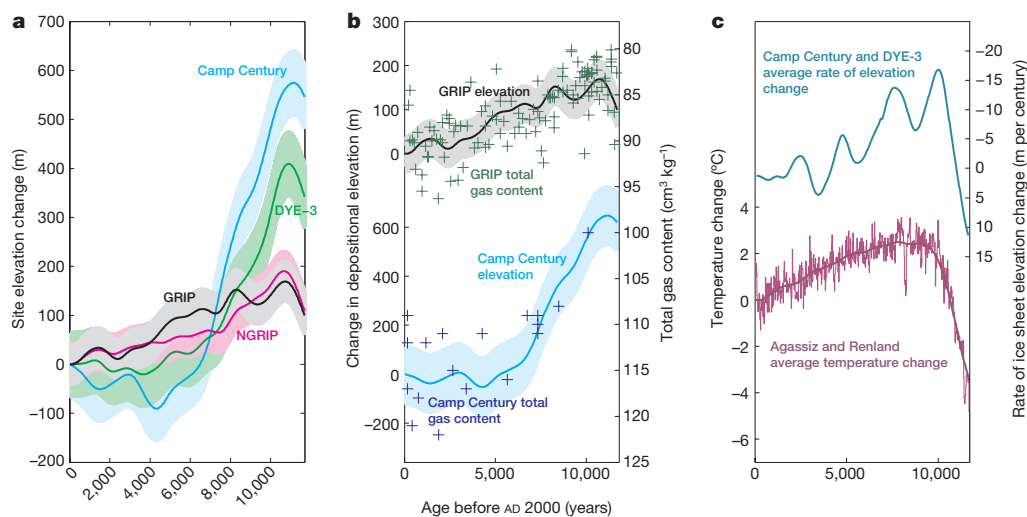


Figure 2 | Holocene elevation change histories for Greenland ice sheet locations. **a**, Changes in elevation at the drill sites, after correction for ice-flow-related upstream effects. The shaded bands show the 1σ uncertainties on the elevation histories. **b**, Depositional elevation histories at the GRIP and Camp Century drill sites compared with total gas measurements

performed on the two ice cores. **c**, Average rate of elevation change of ice sheets at the DYE-3 and Camp Century drill sites compared with temperature change in Greenland derived from Agassiz and Renland $\delta^{18}\text{O}$ records.

from $\delta^{18}\text{O}$ to temperature has been obtained through a calibration with borehole temperatures from the Camp Century, DYE-3, GRIP and NGRIP drill sites²³. The borehole temperature profiles are fully consistent with the Agassiz and Renland average $\delta^{18}\text{O}$ record, supporting our assertion that the climate in and around Greenland was homogeneous during the Holocene (Supplementary Information).

The average rate of elevation change at the Camp Century and DYE-3 drill sites is also shown in Fig. 2c. It can be inferred that elevations at these two sites near the margin of the GIS respond rapidly to Greenland temperature change. The most significant periods of decrease in elevation coincided with the climatic optimum 7–10 kyr before AD 2000. This suggests that the GIS responds significantly to a temperature increase of a few degrees Celsius, even though part of the GIS response in the early Holocene was also associated with ice break-off resulting from rising sea level. The colder climate prevailing during the past two millennia induced a slight increase in elevation of the GIS at these sites.

The 600-m decrease in surface elevation observed at Camp Century in the period from 11 to 6 kyr before AD 2000 can be taken as strong support for the finding that the Hall basin, the Kennedy channel and the Kane basin were completely covered by sheet ice during the earliest Holocene, thereby connecting Greenland to the Innuitian ice sheet on Ellesmere Island^{15,24}. The breakdown of this interconnection and the retreat of the GIS from the continental shelf edge in Melville Bay then led to a significant decrease in surface elevation at Camp Century. At DYE-3, GIS elevation was reduced by about 400 m as the width of the southern GIS probably decreased by one-third during the transition from glacial to Holocene climatic conditions²⁵.

The novel concept of using the combined evidence from Greenland and Canadian ice cores to extract both a Holocene temperature history (Fig. 2c) and Holocene elevation histories (Fig. 2a) for the GIS is essential for the validation of efforts to model the evolution of the GIS. By comparing the results of two conceptual

modelling efforts^{13,26} with the new GRIP Holocene elevation curve it is possible to give a semi-empirical estimate of the position of the GIS margin during the last glaciation, because only a marginal position at the continental shelf edge is consistent with the observed GRIP elevation history (Fig. 3a). A comparison of the GRIP elevation change with more recent state-of-the-art three-dimensional thermomechanical models of ice sheets^{27–30} strongly suggests that none of these models captures the evolution in GRIP elevation during the Holocene (Fig. 3b). The results of the conceptual modelling shown in Fig. 3a indicate that the three-dimensional models fail to advance the GIS sufficiently far onto the continental shelf during the last glaciation, possibly because of an insufficient understanding of interactions between ice sheets and oceans. The poor performance of the three-dimensional models might also be a consequence of similarly simplified climatic forcing series being applied in all model runs, for example an underestimation of the amplitude of the Holocene climatic optimum in Greenland.

The clear Greenland Holocene climatic optimum now unmasked in $\delta^{18}\text{O}$ records from GIS ice cores brings these records into line with borehole temperature data. This rehabilitates $\delta^{18}\text{O}$ as a reliable temperature proxy, paving the way for temperature reconstructions based on high-resolution $\delta^{18}\text{O}$ records from ice cores. The GIS temperature and elevation histories presented here also suggest that the GIS responds more vigorously to climatic change than indicated by the three-dimensional models used for GIS projections. It is therefore entirely possible that a future temperature increase of a few degrees Celsius in Greenland will result in GIS mass loss and contribution to sea level change larger than previously projected.

Received 5 January; accepted 24 July 2009.

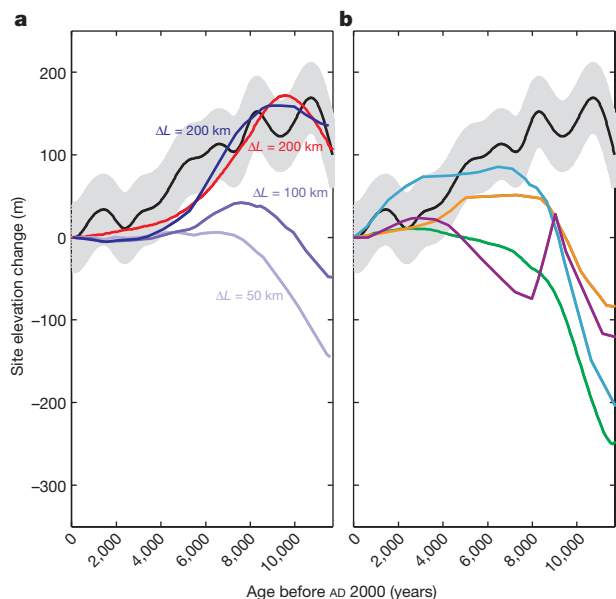


Figure 3 | Empirical and modelled Holocene elevation change histories for the summit of the Greenland ice sheet. a, Elevation change at the GRIP drill site (black line) compared with four different estimates from two different simple models of ice sheets (red line, ref. 26; blue lines, ref. 13). The shaded band shows the 1σ uncertainty in the elevation history. The modelled estimates are based on three different assumed maximum advances (ΔL) of the margin of the Greenland ice sheet during the Last Glacial Maximum. **b**, Change in elevation at the GRIP drill site (black line) compared with elevation estimates from four different complex three-dimensional thermomechanical models of ice sheets (orange, ref. 27; magenta, ref. 28; green, ref. 29; turquoise, ref. 30). The shaded band shows the 1σ uncertainty in the elevation history.

- Alley, R. B. *et al.* Ice-sheet and sea-level changes. *Science* **310**, 456–460 (2005).
- Rignot, E. & Kanagaratnam, P. Changes in the velocity structure of the Greenland Ice Sheet. *Science* **311**, 986–990 (2006).
- Johnsen, S. J. & Vinther, B. M. in *Encyclopedia of Quaternary Science* (ed. Elias, S.) Vol. 2, 1250–1258 (Elsevier, 2007).
- Kaufman, D. S. *et al.* Holocene thermal maximum in the western Arctic (0–180°W). *Quat. Sci. Rev.* **23**, 529–560 (2004).
- Fisher, D. A. *et al.* Inter-comparison of ice core $\delta^{18}\text{O}$ and precipitation records from sites in Canada and Greenland over the last 3500 years and over the last few centuries in detail using EOF techniques. *NATO ASI Ser.* **141**, 297–328 (1996).
- Masson-Delmotte, V. *et al.* Holocene climatic changes in Greenland: different deuterium excess signals at Greenland Ice Core Project (GRIP) and NorthGRIP. *J. Geophys. Res.* **110**, D14102 (2005).
- Raynaud, D. & Lorius, C. Climatic implications of total gas content in ice at Camp Century. *Nature* **243**, 283–284 (1973).
- Koerner, R. M. & Fisher, D. A. A record of Holocene summer climate from a Canadian high-Arctic ice core. *Nature* **343**, 630–632 (1990).
- Rasmussen, S. O. *et al.* A new Greenland ice core chronology for the last glacial termination. *J. Geophys. Res.* **111**, D06102. doi:10.1029/2005JD006079 (2006).
- Vinther, B. M. *et al.* A synchronized dating of three Greenland ice cores throughout the Holocene. *J. Geophys. Res.* **111**, D13102. doi:10.1029/2005JD006921 (2006).
- Vinther, B. M. *et al.* Synchronizing ice cores from the Renland and Agassiz ice caps to the Greenland Ice Core Chronology. *J. Geophys. Res.* **113**, D08115. doi:10.1029/2007JD009143 (2008).
- Hammer, C. U. *et al.* Greenland ice sheet evidence of post-glacial volcanism and its climatic impact. *Nature* **288**, 230–235 (1980).
- Cuffey, K. M. & Clow, G. D. Temperature, accumulation, and ice sheet elevation in central Greenland through the last deglacial transition. *J. Geophys. Res.* **102**, 26383–26396 (1997).
- Johnsen, S. J. *et al.* A deep ice core from east Greenland. *Meddr Grøn.* **29**, 3–29 (1992).
- Blake, W. Jr. Studies of glacial history in Arctic Canada. I. Pumice, radiocarbon dates and differential post-glacial uplift in the eastern Queen Elizabeth Islands. *Can. J. Earth Sci.* **7**, 634–664 (1970).
- Funder, S. Holocene stratigraphy and vegetation history in the Scoresby Sund area, East Greenland. *Grøn. Geol. Unders. Bull.* **129** (1978).
- Dyke, A. S. & Peltier, W. R. Forms, response times and variability of relative sea-level curves, glaciated North America. *Geomorphology* **32**, 315–333 (2000).
- Laskar, J. *et al.* A long term numerical solution for the insolation quantities of Earth. *Astron. Astrophys.* **428**, 261–285 (2004).
- Buchardt, S. L. & Dahl-Jensen, D. Estimating the basal melt rate at NorthGRIP using a Monte Carlo technique. *Ann. Glaciol.* **45**, 137–142 (2007).
- Reeh, N. *et al.* Dating the Dye-3 ice core by flow model calculations. *Am. Geophys. Un. Geophys. Monogr.* **33**, 57–65 (1985).

21. Raynaud, D. *et al.* Air content along the Greenland Ice Core Project core: a record of surface climatic parameters and elevation in central Greenland. *J. Geophys. Res.* **102**, 26607–26613 (1997).
22. Waelbroeck, C. *et al.* Sea-level and deep water temperature changes derived from benthic foraminifera isotopic records. *Quat. Sci. Rev.* **21**, 295–305 (2002).
23. Dahl-Jensen, D. *et al.* Past temperatures directly from the Greenland ice sheet. *Science* **282**, 268–271 (1998).
24. Blake, W. & Jr.. Glaciated landscapes along Smith Sound, Ellesmere Island, Canada and Greenland. *Ann. Glaciol.* **28**, 40–46 (1999).
25. Long, A. J. *et al.* Late Weichselian relative sea-level changes and ice sheet history in southeast Greenland. *Earth Planet. Sci. Lett.* **272**, 8–18 (2008).
26. Johnsen, S. J. *et al.* Greenland palaeotemperatures derived from GRIP bore hole temperature and ice core isotope profiles. *Tellus B* **47**, 624–629 (1995).
27. Huybrechts, P. Sea-level changes at the LGM from ice-dynamic reconstructions of the Greenland and Antarctic ice sheets during the glacial cycles. *Quat. Sci. Rev.* **21**, 203–231 (2002).
28. Tarasov, L. & Peltier, W. R. Greenland glacial history, borehole constraints and Eemian extent. *J. Geophys. Res.* **108** (B3), 2124–2143 (2003).
29. Greve, R. Relation of measured basal temperatures and the spatial distribution of the geothermal heat flux for the Greenland ice sheet. *Ann. Glaciol.* **42**, 424–432 (2005).
30. Lhomme, N. *et al.* Tracer transport in the Greenland Ice Sheet: constraints on ice cores and glacial history. *Quat. Sci. Rev.* **24**, 173–194 (2005).

Supplementary Information is linked to the online version of the paper at www.nature.com/nature.

Acknowledgements We thank laboratory technician A. Boas, who meticulously performed most of the stable-isotope measurements presented in this paper during her 38 years at the Copenhagen stable isotope laboratory; W. Blake Jr for providing his insight, suggestions and corrections during the drafting of this paper; R. Greve for providing elevation data from his GIS modelling effort. B.M.V. thanks the Carlsberg Foundation for funding, and the Climatic Research Unit at University of East Anglia for hosting his research during all of 2007. V.L. and D.R. thank the Groupement de Recherche Européen (GDRE) Vostok (Institut national des sciences de l'Univers (INSU)/Centre national de la recherche scientifique (CNRS) for funding and Russian Foundation for Basic Research (RFBR)–CNRS grant 05-05-66801 for support.

Author Information Reprints and permissions information is available at www.nature.com/reprints. Correspondence and requests for materials should be addressed to B.M.V. (bo@gfy.ku.dk).